


# Carbon sequestration capacity and productivity responses of Mediterranean olive groves under future climates and management options

L. Brilli<sup>1,2</sup>  · E. Lugato<sup>3</sup> · M. Moriondo<sup>1</sup> · B. Gioli<sup>1</sup> · P. Toscano<sup>1</sup> · A. Zaldei<sup>1</sup> · L. Leolini<sup>2</sup> · C. Cantini<sup>4</sup> · G. Caruso<sup>5</sup> · R. Gucci<sup>5</sup> · P. Merante<sup>1</sup> · C. Dibari<sup>2</sup> · R. Ferrise<sup>2</sup> · M. Bindi<sup>2,6</sup> · S. Costafreda-Aumedes<sup>2</sup>

Received: 8 May 2018 / Accepted: 29 June 2018  
© Springer Nature B.V. 2018

**Abstract** The need to reduce the expected impact of climate change, finding sustainable ways to maintain or increase the carbon (C) sequestration capacity and productivity of agricultural systems, is one of the most important challenges of the twenty-first century. Olive (*Olea europaea* L.) groves can play a fundamental role due to their potential to sequester C in soil and woody compartments, associated with widespread cultivation in the Mediterranean basin. The implementation of field experiments to assess olive grove responses under different conditions, complemented by simulation models, can be a powerful approach to explore future land-atmosphere C feedbacks. The DayCent biogeochemical model was calibrated and validated against observed net ecosystem exchange, net primary productivity, aboveground biomass, leaf area index, and yield in two Italian olive groves. In addition, potential changes in C-sequestration capacity and productivity were assessed under two types of management (extensive and intensive),

**Electronic supplementary material** The online version of this article (<https://doi.org/10.1007/s11027-018-9824-x>) contains supplementary material, which is available to authorized users.

✉ L. Brilli  
l.brilli@ibimet.cnr.it; lorenzo.brilli@unifi.it

<sup>1</sup> IBIMET-CNR, Via G. Caproni 8, 50145 Florence, Italy

<sup>2</sup> DiSPAA, University of Florence, Piazzale delle Cascine 18, 50144 Florence, Italy

<sup>3</sup> European Commission, Joint Research Centre (JRC), Directorate for Sustainable Resources, Land Resources Unit, Via E. Fermi 2749, 21027 Ispra, VA, Italy

<sup>4</sup> IVALSÀ-CNR, Via Aurelia 49, 58022 Follonica, GR, Italy

<sup>5</sup> Dipartimento di Scienze Agrarie, Alimentari e Agro-ambientali (DiSAAA-a), Università di Pisa, Via del Borghetto 80, 56124 Pisa, Italy

<sup>6</sup> Unità di ricerca Cambiamenti Climatici, Sistemi ed Ecosistemi, Piazzale delle Cascine 18, 50144 Florence, Italy

35 climate change scenarios ( $\Delta T$ -temperature from +0 °C to +3 °C;  $\Delta P$ -precipitation from 0.0 to -20%), and six areas across the Mediterranean basin (Brindisi, Coimbra, Crete, Cordoba, Florence, and Montpellier). The results indicated that (i) the DayCent model, properly calibrated, can be used to quantify olive grove daily net ecosystem exchange and net primary production dynamics; (ii) a decrease in net ecosystem exchange and net primary production is predicted under both types of management by approaching the most extreme climate conditions ( $\Delta T = +3$  °C;  $\Delta P = -20\%$ ), especially in dry and warm areas; (iii) irrigation can compensate for net ecosystem exchange and net primary production losses in almost all areas, while ecophysiological air temperature thresholds determine the magnitude and sign of C-uptake; (iv) future warming is expected to modify the seasonal net ecosystem exchange and net primary production pattern, with higher photosynthetic activity in winter and a prolonged period of photosynthesis inhibition during summer compared to the baseline; (v) a substantial decrease in mitigation capacity and productivity of extensively managed olive groves is expected to accelerate between +1.5 and +2 °C warming compared to the current period, across all Mediterranean areas; (vi) adaptation measures aimed at increasing soil water content or evapotranspiration reduction should be considered the mostly suitable for limiting the decrease of both production and mitigation capacity in the next decades.

**Keywords** *Olea europaea* · DayCent · Climate change · Mitigation · Productivity

## 1 Introduction

Olive (*Olea europaea* L.) can be considered the most representative tree cultivation across Mediterranean countries. This agroecosystem plays a key role especially in marginal regions with low productivity (mountainous or hilly areas), where high-value food commodities contribute to maintaining a suitable income for local farming communities (Oxfam 2010; Mohamad et al. 2013; Testa et al. 2014). Production systems encompass both traditional rainfed olive groves, usually in mountainous or hilly areas, and intensive systems with the use of irrigation and a high level of mechanization. Olive groves also provide several ecosystem services such as environmental conservation, landscape ecology, biodiversity, and climate mitigation (Sofa et al. 2005; Prabhakaran Nair 2010; Maselli et al. 2012).

Interest in olive grove response to climate change has recently been increasing because of the ability of this system to sequester carbon (C) in soil and woody compartments (Nieto et al. 2010; Montanaro et al. 2018), associated with a widespread and economically worthwhile cultivation in the Mediterranean basin. The significant warming associated with a 25 to 30% reduction in precipitation expected over the Mediterranean basin (Giorgi and Lionello 2008; IPCC 2013) may negatively impact both yield and C-sequestration capacity with detrimental effects for both farmer income and climate mitigation potential.

However, because of the interaction among multiple drivers, understanding the level at which climate change will affect the yield and C-sequestration capacity of olive groves is very difficult. In rainfed Mediterranean environments, the magnitude of C-fluxes is particularly associated with precipitation patterns and timing (Noy-Meir 1973; Chaves et al. 2002; Kwon et al. 2008; Medrano et al. 2009; Jia et al. 2014; Brilli et al. 2016), while biomass production and yield can vary based on the management adopted (e.g., irrigation vs rainfed, tillage vs no tillage, grass cover vs bare soil) (Gucci et al. 2012; Nardino et al. 2013; Brilli et al. 2013, Scandellari et al. 2016; Chamizo et al. 2017).

Given the broad variability of systems (agroforestry stands, traditional groves, new intensive orchards), environments (climate, soil characteristics), and managements, field experiments for assessing olive grove responses under the whole range of conditions are challenging and may likely require high investment costs.

These limitations may be overcome using simulation models that can investigate the response of cropping systems under different soil, management (Smith et al. 2002; del Grosso et al. 2005; Tonitto et al. 2007; Lugato et al. 2010, 2018; Sándor et al. 2016), and climate conditions (Graux et al. 2009; Abdalla et al. 2010; Vital et al. 2013; Graux et al. 2013). Many of these tools incorporate a relatively complete array of physiological and biogeochemical processes (e.g., plant growth, C decomposition, N transformation), which allow computation of plant–soil ecosystem processes at different time and space scale (Brilli et al. 2017; Ehrhardt et al. 2018). Although several biophysical and biogeochemical models have been applied on forests and arable systems, only a few have been used on olive groves (Alvaro-Fuentes et al. 2012; Gargouri et al. 2013; Lugato et al. 2014; Moriondo et al. 2015); in addition, to our knowledge, no study has been conducted on olive groves to simulate the net ecosystem exchange (NEE) and the net primary production (NPP) at a daily step.

The main objective of this work was to assess the potential change in C-sequestration capacity and yield of a typical Mediterranean olive grove under two types of management (intensive and extensive), 35 climate change scenarios and 6 areas across the Mediterranean basin (Brindisi (IT), Coimbra (P), Crete (GR), Cordoba (SP), Florence (IT) and Montpellier (FR)), using the biogeochemical model DayCent (Parton et al. 1994, 1998). The model was first specifically calibrated and validated in two sites against eddy covariance flux measurements and olive tree aboveground biomass and yield. In this study, the NEE was used as indicator of olive grove C-sequestration capacity, and the NPP as a proxy for yield. Potential change in C-sequestration capacity and productivity were assessed using impact response surfaces (IRSs), with a focus on the two goals of the Paris Climate Agreement: “holding the increase in the global average temperature to well below 2 °C above pre-industrial levels and pursuing efforts to limit the temperature increase to 1.5 °C” (UNFCCC 2015).

## 2 Materials and methods

### 2.1 Calibration and validation sites

Two olive groves located in central Italy were used as calibration/validation sites for the modeling exercise. The sites were located in Tuscany, one of the most important olive cultivation regions, thus to be considered highly representative of typical Mediterranean olive groves.

1. Site 1 (Follonica, 42°56'N, 10°46'E) was used for model calibration (2010) and validation (2011–2012) against eddy covariance data. The olive grove covers more than 6 ha with over 1500 plants at 7 × 5 m spacing (low plant density) with average canopy height of 5.5 m, covering about 25% of the ground (Maselli et al. 2012). Olive leaf area index (LAI) was equal to 1. Total fruit production was retrieved for the period 1999–2006 and 2010–2012. Harsh weather conditions coupled with alternate fruit bearing caused unharvesting

in 2011. The soil has a clay-sand texture, pH of 7, and bulk density of  $1.27 \text{ Mg m}^{-3}$ . The available water content was estimated to range from 60 to  $90 \text{ mm m}^{-1}$ . The local climate is characterized by mild winter and high temperatures and prolonged drought periods during summer. Total precipitation is around  $600 \text{ mm year}^{-1}$  on average with a typical Mediterranean seasonal distribution (for details, see Brillì et al. 2016).

2. Site 2 (Venturina,  $42^{\circ}01'N$ ,  $10^{\circ}36'E$ ) was used to further validate DayCent model against inventorial measurements. The olive grove (*Olea europaea* L. cv. Frantoio) was planted at a density of  $513 \text{ trees ha}^{-1}$  in April 2003 at the University of Pisa experimental farm. The soil is a Typic Haploxeralf, coarse-loamy, mixed, thermic (Soil Survey Staff 2010), 1.5 m deep, with sandy loam texture (Gucci et al. 2012). Meteorological data were acquired from a weather station located in the grove (Pessl Instruments GmbH, Weiz, Austria) (Caruso et al. 2013; Caruso et al. 2014). The grove was divided into three randomly distributed blocks, each consisting of three irrigation treatments: fully irrigation (100% of ETc), deficit irrigation (46–48% of ETc), and rainfed. The aboveground biomass and LAI, used for model validation, were determined for 2008, 2009, and 2010. For further details, see Scandellari et al. (2016).

## 2.2 Alternative management scenarios across the Mediterranean region

To assess the impact of future climate variability on the current olive grove C-sequestration capacity and productivity in the Mediterranean region, six representative areas were chosen: Brindisi and Florence (Italy), Coimbra (Portugal), Cordoba (Spain), Crete (Greece), Montpellier (France) (Fig. 1). For each area, two different agronomic scenarios and one soil type were used (Table 1). Given the broad variability of timing and management inputs of this agroecosystem, the two agronomic scenarios used in this study were built to generally reflect traditional and modern-intensive cultivations, namely extensive (EXT) and intensive (INT). The soil was built to reflect a well-balanced soil (medium texture) in order to simulate the best soil condition for all sites (e.g., good water infiltration, aeration, moisture content). This allowed the impact of only climate variability on olive grove C-sequestration capacity and productivity to be pointed out, avoiding coupling effects with different soil characteristics among sites.

## 2.3 Meteorological data and future climate scenarios

Three meteorological datasets were used: (i) ancillary measurements from the two local stations (daily minimum (Tmin) and maximum (Tmax) air temperature, precipitation (P), and global radiation) were used for calibrating and validating DayCent; (ii) data from the European climate assessment and dataset (ECA&D) ([www.ecad.eu/](http://www.ecad.eu/)) archive were used for the long-term climate characterization (1971–2000) of the six testing areas; (iii) 300 years of synthetic weather data from the latest version (ver 5.5) of the weather generator LARS-WG (Semenov and Barrow 1997; Semenov and Stratonovitch 2010) were used to create the baseline scenarios (Tmax, Tmin and P) at daily time step for the six testing areas. These data were then perturbed by increasing the daily Tmax and Tmin between  $+0 \text{ }^{\circ}\text{C}$  and  $+3 \text{ }^{\circ}\text{C}$  at  $0.5 \text{ }^{\circ}\text{C}$  intervals ( $\Delta T$ ), and P between 0.0 and  $-20\%$  at  $5\%$  ( $\Delta P$ ) intervals. These temperature increases are consistent with projections of the highest reference concentration pathway (RCP8.5) from the multimodel ensemble CMIP5 datasets (Collins et al. 2013).

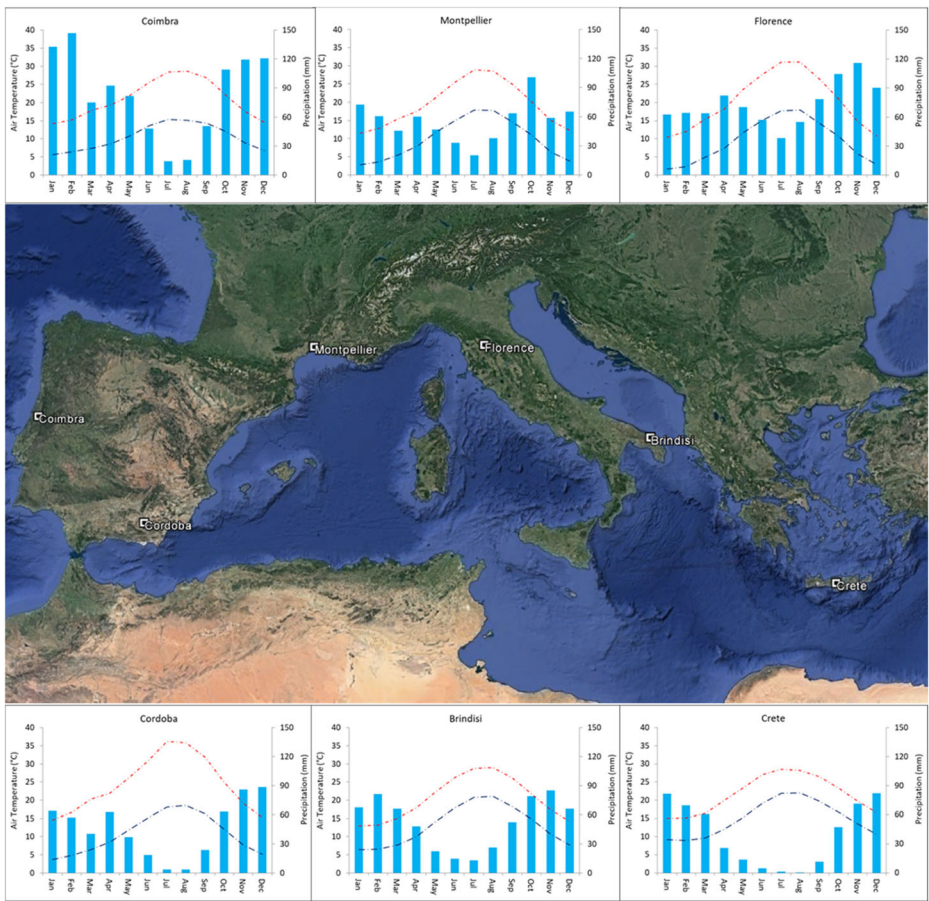


**Fig. 1** Ikonos Panel Sharp (IPS) image from Google Earth showing Mediterranean basin and the position of the six test sites. Above and below the IPS image the 30-year climate courses (monthly maximum and minimum air temperature (°C) and precipitation (mm)) are reported for each site. Source: Google Earth

## 2.4 Eddy covariance data acquisition and processing

The eddy covariance (EC) micrometeorological technique was applied to measure carbon dioxide (CO<sub>2</sub>) and energy exchanges (i.e., sensible heat (H), and latent heat (LE)) between ecosystem and atmosphere (Baldocchi et al. 1996) at the Follonica site. The EC station was installed in the central part of the olive grove to maximize spatial coverage of measurements. The fast response sensors (i.e., a Metek USA 1 triaxial sonic anemometer and a Licor 7500 open path infra-red CO<sub>2</sub>-H<sub>2</sub>O analyzer) were placed at 7 m in height from the ground and about 2 to 3 m above the canopy. Data from sensors were acquired at high frequency (20 Hz) and then stored on a portable laptop. Ancillary data included half-hourly measurements of soil temperature from 5 to 20 cm (thermocouples J and T types), air temperature and humidity (HMP45 Vaisala), global and net radiation (CMP3 and NR LITE Kipp & Zonen), and rainfall (Davis 7852 rain gauge). All binary files and meteorological data collected by the EC tower were stored on a data logger

**Table 1** Agronomic scenarios and soil type used for each simulated Mediterranean site

Management		Soil characteristics		Fertilization <sup>a</sup>		Tillage <sup>b</sup>		Irrigation <sup>c</sup>		Cutting <sup>d</sup>		Pruning <sup>e</sup>	
Type	Extensive	Grove density (> 300 trees ha <sup>-1</sup> ) (< 300 trees ha <sup>-1</sup> )	Field capacity (%)	150 kg N ha <sup>-1</sup> 80 kg N ha <sup>-1</sup>	Harrowing Harrowing	Full Rainfed	Inter-row N/A	Crown and leaves Crown and leaves					
Bulk density (g/cm <sup>3</sup> )	1.43	29	45	Sand (%)	Silt (%)	OM (%)	Saturated Hydraulic Conductivity (cm/s <sup>-1</sup> )	pH					
				45	30	2	0.00027	7					

<sup>a</sup> Ammonium nitrate was spread on the soil in early spring (March 31st)

<sup>b</sup> Inter-row harrowing (superficial tillage 5 cm depth) was done twice per year, in spring (May 5th) and early summer (July 10th)

<sup>c</sup> One irrigation at field capacity was performed every week from mid-May to the end of July and during the first two weeks of September

<sup>d</sup> Inter-row vegetation was removed once a year at the end of spring (May 31st) and left to decay on the soil surface

<sup>e</sup> One pruning operation of leaves and fine branches was done in mid-winter (January 30th). The pruning residues were removed from fields

(Campbell CR10X) and then processed by the Eddy Pro® Software ([https://www.licor.com/env/products/eddy\\_covariance/eddypro.html](https://www.licor.com/env/products/eddy_covariance/eddypro.html)). Final outputs from Eddy Pro® consisted of NEE data at half-hourly resolution. These data were then processed using Reichstein et al. (2005) (<http://www.bgc-jena.mpg.de/~MDIwork/eddyproc/>) in order to partition the net flux into the main components, namely gross primary production (GPP) and ecosystem respiration (Reco). For uncertainties correction, footprint analysis and data coverage percentage see Brilli et al. (2016).

## 2.5 DayCent description, simulation setup, and run

DayCent, the daily time step version of the biogeochemical Century model (Parton et al. 1994, 1998), was designed to simulate soil C dynamics, nutrient flows (nitrogen (N), phosphorus (P), sulfur (S)), and trace gas fluxes (CO<sub>2</sub>, CH<sub>4</sub>, N<sub>2</sub>O, NO<sub>x</sub>, N<sub>2</sub>) between soil, plants, and the atmosphere (Parton et al. 1998, del Grosso et al. 2001a, b). The model was used for the following reasons: (i) it takes into account the effect of tree canopy cover on grassland production, N competition between the two vegetation layers, and the effects of different agronomic practices (pruning, tillage, mowing, fertilization) driving C-dynamics, thus resulting as a suitable tool for reproducing NEE and NPP in complex ecosystems, including savannas; (ii) it is able to simulate the effects of elevated CO<sub>2</sub> and other global changes on net primary production, transpiration rate, and C/N ratio in biomass, thus being a highly suitable tool for predicting the GHG mitigation potential of different management systems under future scenarios (De Gryze et al. 2010).

Simulation set-up included weather, soil, vegetation, and management implementation. The weather variables included daily minimum and maximum air temperature, precipitation, and solar radiation. According to the BERN-CC model for the A1B projections at 2050, the CO<sub>2</sub> concentration was set to 400 ppm for the baseline and 550 ppm for increased temperature scenarios. Soil characteristics were based on field data collected within the test sites. The vegetation ecophysiological characteristics were initially set according to default values found for Mediterranean mixed grass and evergreen trees. Management practices for spin-up and current period were set to reflect as closely as possible the historical and current land use, vegetation type, and management. The spin-up for setting up initial conditions of the main state variables (e.g., carbon and nitrogen pool sizes) for calibration and test sites consisted of almost 2000 years of continuous forest (1–1924), followed by a low yield wheat monoculture (1925–1951) and woody systems (1952–2010).

Once implemented, DayCent was calibrated and validated following three steps: (1) sensitivity analysis to detect the most relevant parameters controlling the NEE and GPP. The most sensitive inputs were identified manually changing one input parameter at each run, thus determining the magnitude of changes in the outputs; (2) calibration of the most important parameters identified with sensitivity analysis, minimizing the root mean square error (RMSE) between observed and simulated data of daily NEE and GPP at Follonica site for 2010; (3) validation against daily NEE and GPP at Follonica site for 2011 and 2012, aboveground biomass and LAI with three types of management for the period 2008–2010 at Venturina (site 2) and yield at both sites for the period 1999–2012. Yields were calculated using a potential harvest index of 0.35 on olive tree biomass (expressed as dry matter, DM) (Villalobos et al. 2006). To limit the effect of alternate bearing, yields were averaged over 2 years.

## 2.6 Impact response surfaces

The impact response surfaces (IRSs) is a statistical methodology showing the response of an impact variable to changes in two explanatory variables (here, precipitation and temperature). These surfaces are built by plotting the results of first- and second-order function (Lenth 2009; Wu and Hamada 2009) outcomes of the predictors to the response variable changes. This methodology has been widely applied by several modeling studies (Fronzek et al. 2010; Pirttioja et al. 2015, Ruiz-Ramos et al. 2018). In this study, IRSs were generated using 100 years of outcomes at yearly and monthly time-step of four variables (i.e. GPP, NEE, NPP and Reco) for each management and location. Only yearly IRSs are reported here, while monthly IRSs were used to summarize the monthly tendency of each variable to  $\Delta P$  and  $\Delta T$  changes. The monthly tendency was calculated identifying the direction of the maximum variation rate (i.e., slope direction) from each IRS pixel to its neighbors. IRSs were created using “rsm” package (Lenth 2009) in the statistical software environment R (<http://www.R-project.org/>).

## 2.7 Statistical analysis

Correlation coefficients ( $r$ ) and root mean square error (RMSE) of observed and simulated data were calculated to assess model accuracy. All statistics were applied at different time scales (daily, 10 days, and monthly). Uncertainties associated to each average value were computed as 95% confidence intervals assuming a Gaussian distribution. IRSs were used to assess changes in yearly dynamics of productivity and C-sequestration capacity among the baseline and different scenarios. The IRSs were built using the last 100 runs of the model for each scenario considered, averaging the data across years.

# 3 Results

## 3.1 Climate trend

The six study areas reflected the typical climatic trend of a Mediterranean environment, with clear differences in the long-term seasonal and annual regimes (Fig. 1). Average yearly rainfall differed across sites: Coimbra (1005 mm) and Florence (880 mm) were the wettest, Crete was the driest (471 mm). The other sites showed a yearly average of about 600 mm. The highest rainfall was concentrated in spring (April–May) and late autumn (October–November).

The highest air temperatures were in July and August at Cordoba (average maximum of 36 °C) and Florence (average maximum of 31.2 °C), the lowest in January at Florence (average minimum of 10.1 °C) and Montpellier (average minimum of 11.5 °C).

## 3.2 Model sensitivity

The sensitivity analysis indicated that the most relevant parameters controlling NEE and GPP (derived from simulated NPP by using the NPP/GPP ratio reported by Zhang et al. 2009 for shrub-evergreen ecosystems) resulted as being those related to plant production and water and nutrient availability, plant density and canopy cover effect, C allocation to plant organs, and decomposition processes. Once identified, these parameters were calibrated in a range derived



from the literature, DayCent handbook (<https://www.nrel.colostate.edu/projects/century/index.php>) and Zhou et al. (2007) (Table S1).

For olive trees, the potential aboveground monthly production (PRDX(1)) was reduced from 0.5 to 0.23. The optimum and maximum air temperature for biomass production and growth were reduced from a default value of 27 to 23 °C and from 36 to 35 °C, respectively, while the number of soil layers used to determine water and nutrients available for crop growth was changed from 5 (30 cm soil depth) to 8 (75 cm). The biomass partitioning among the five tree compartments (leaves, fine branches, large wood, fine, and coarse roots) was calibrated changing the C allocation due to new production (fcfrac) and its response to water and nutrient stress (tfrtc). The conversion factor from biomass to LAI was changed from 0.008 to 0.007 while the maximum C/N ratio in leaves was increased from 60 to 90. The maintenance respiration for large wood and coarse roots was reduced from 0.01525 to 0.0045. Lastly, the ratio between basal area and wood biomass (basfct), the parameter relating tree basal area to grass N fraction (basfc2), the multiplier for the equation to dynamically compute the aboveground herbaceous layer production in the absence of trees (sitpot), and the theoretical maximum LAI achievable in a mature forest were set to reproduce the olive grove characteristics (medium-low density, < 300 plants/ha).

For mixed grasses, the coefficient for calculating potential aboveground monthly production (PRDX(1)) was set to 0.3. The optimum and maximum air temperature for grass growth were decreased from 22 to 18 °C and from 34 to 26 °C, respectively. The number of soil layers used to determine water and mineral N, P, and S that are available for crop growth were increased from 2 to 4 (from 5 to 30 cm).

### 3.3 Model calibration and validation

The daily patterns of NEE and GPP simulated by the model at daily time steps during 2010 were very close to those measured in the field (Fig. 2, negative values indicate a C sink whilst positive values indicate net CO<sub>2</sub> emissions). Cumulative NEE simulated by the model for the period March–December of 2010 ( $-616 \text{ gC m}^{-2} \text{ year}^{-1}$ ) was only 5% lower than that measured ( $-647.2 \pm 25.4 \text{ gC m}^{-2} \text{ year}^{-1}$ ), while simulated GPP ( $1190.2 \text{ gC m}^{-2} \text{ year}^{-1}$ ) was almost the same as the measured value ( $1179 \pm 25.7 \text{ gC m}^{-2} \text{ year}^{-1}$ ).

Model validation over 2011–2012 confirmed the capacity of the model to reproduce the C-flux dynamics in the grove (Fig. 3a, b and Table 2). In 2011, the biggest differences between simulated and measured fluxes were detected during early spring, when the model tended to overestimate the NEE. Cumulated yearly NEE simulated by the model ( $-384.7 \text{ gC m}^{-2} \text{ year}^{-1}$ ) was higher than that measured ( $-149.3 \pm 13.2 \text{ gC m}^{-2} \text{ year}^{-1}$ ), while the simulated GPP (897.7) was virtually the same as the measured one ( $875.8 \pm 12.4 \text{ gC m}^{-2} \text{ year}^{-1}$ ). In 2012 (February–September), the model was able to simulate the measured daily GPP and NEE pattern (Table 2). Cumulative simulated NEE ( $-181.5 \text{ gC m}^{-2} \text{ year}^{-1}$ ) and GPP ( $494.5 \text{ gC m}^{-2} \text{ year}^{-1}$ ) were 17 and 21% lower than that observed (i.e.  $-218.3 \pm 11.2$  and  $624.9 \pm 13.1 \text{ gC m}^{-2}$ ). Based on the whole study period, the simulated NEE ( $-1182.2 \text{ gC m}^{-2}$ ) and GPP ( $2500.0 \text{ gC m}^{-2}$ ) were very close to the measured values and always within the experimental variability of measured data (Fig. 3a, b). The cumulated patterns over the whole study period confirmed the good model performances at reproducing olive grove C-fluxes (Fig. 3c).

Model validation against LAI and aboveground biomass showed some contrasting results. Aboveground biomass was well simulated by the model (Fig. 4a), with almost no differences between simulated and measured data. By contrast, the simulated LAI reproduced the

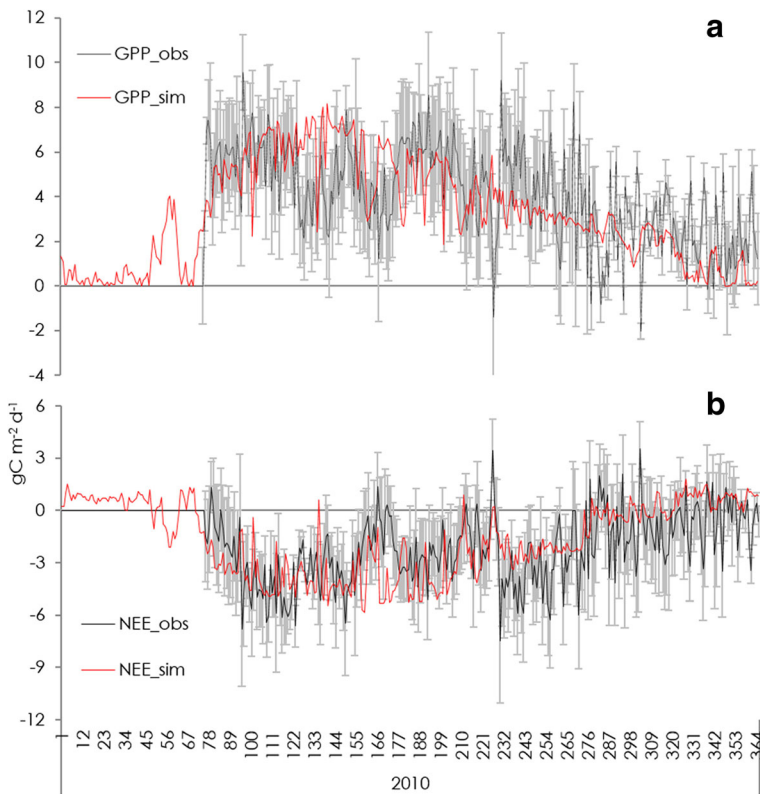


**Fig. 2** Simulated (red line) and measured (black line) daily patterns of GPP (**a**) and NEE (**b**) in 2010. Vertical bars represent 95% confidence interval of the mean

observed climate and management variations, but did not cover the whole variability range, showing a flatter pattern compared to the observed (Fig. 4b). Lastly, the model was validated against actual yields at Follonica and Venturina from 1999 to 2012. Statistics confirmed the DayCent reliability in reproducing yields under different environmental (i.e., soil and climate) and management conditions.

### 3.4 Impact response surfaces: net ecosystem exchange and net primary production response

Under extensive management, the yearly mean values of olive grove NEE (Fig. 5a) showed a continuous decrease of C-sequestration capacity from the baseline by increasing temperature and decreasing precipitation, varying in magnitude among the sites. The highest NEE reductions were observed under the extreme climate scenario ( $\Delta T = +3$  °C;  $\Delta P = -20\%$ ) for all sites. Here, the lowest decrease was found at Coimbra ( $-15\%$ ) and Florence ( $-40\%$ ), the highest at Cordoba ( $-140\%$ ). The patterns of isolines differed among the sites. At Coimbra and Florence, the wettest sites, the isolines were almost vertical, thus indicating the main role of temperature in controlling NEE decrease. By contrast, at Brindisi, Cordoba, and Crete, the isoline patterns suggested the main role of precipitation in controlling NEE decrease, while at Montpellier, they indicated a similar relative importance of precipitation and temperature.

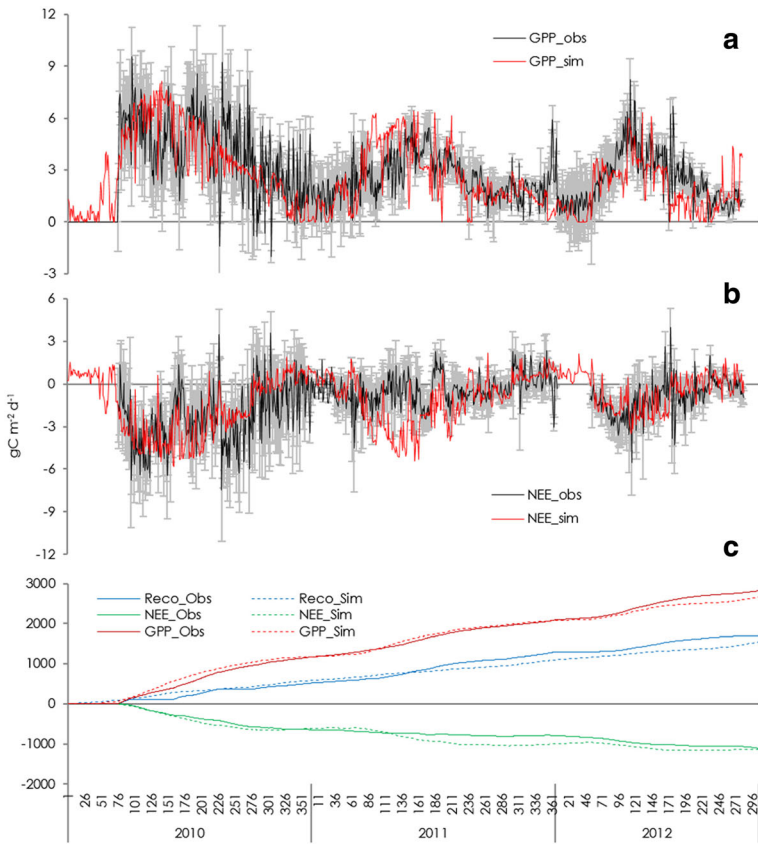


**Fig. 3** Simulated (red line) and observed (black line) daily pattern of GPP (a) and NEE (b) and cumulated pattern (c) of simulated (dashed line) and observed (full line) GPP (red line), NEE (green line), and Reco (blue line) during the period 2010–2012. Vertical bars represent 95% confidence interval of the mean

**Table 2** Statistics (r and RMSE) of model calibration (2010) and validation (2011, 2012) reported for GPP and NEE calculated for single years and over the whole period (2010–2012) using different time steps

Year	Time-step	GPP		NEE	
		r	RMSE	r	RMSE
2010	Daily	0.66	2.39	0.59	2.04
	10 days	0.84	21.32	0.82	17.29
	Monthly	0.87	61.51	0.87	50.50
2011	Daily	0.41	1.47	0.24	1.46
	10 days	0.56	13.11	0.31	12.58
	Monthly	0.74	35.79	0.44	34.82
2012	Daily	0.60	1.49	0.45	1.24
	10 days	0.83	13.65	0.73	9.31
	Monthly	0.92	42.69	0.86	25.55
2010–2012	Daily	0.60	2.00	0.46	1.74
	10 days	0.78	17.39	0.66	14.51
	Monthly	0.86	52.01	0.73	41.56

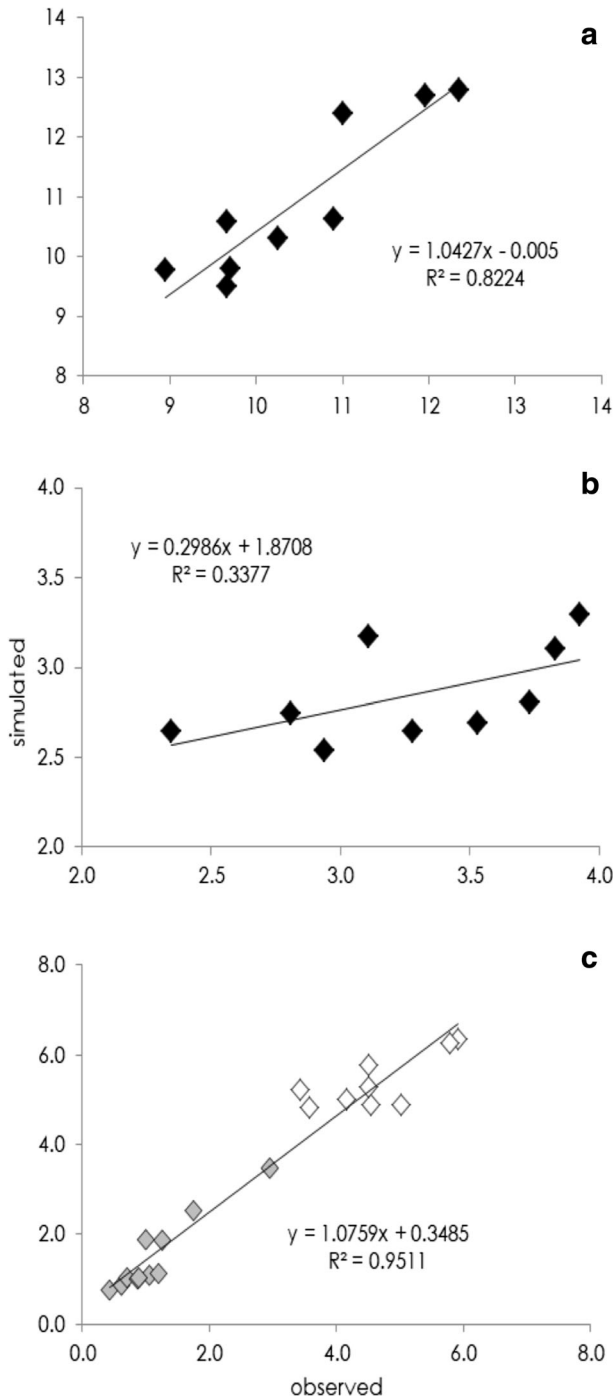


**Fig. 4** Simulated and measured. **a** Aboveground biomass (tDM/ha). **b** LAI. **c** Yield (tDM/ha). White and gray diamonds were yields simulated at Venturina and Follonica, respectively

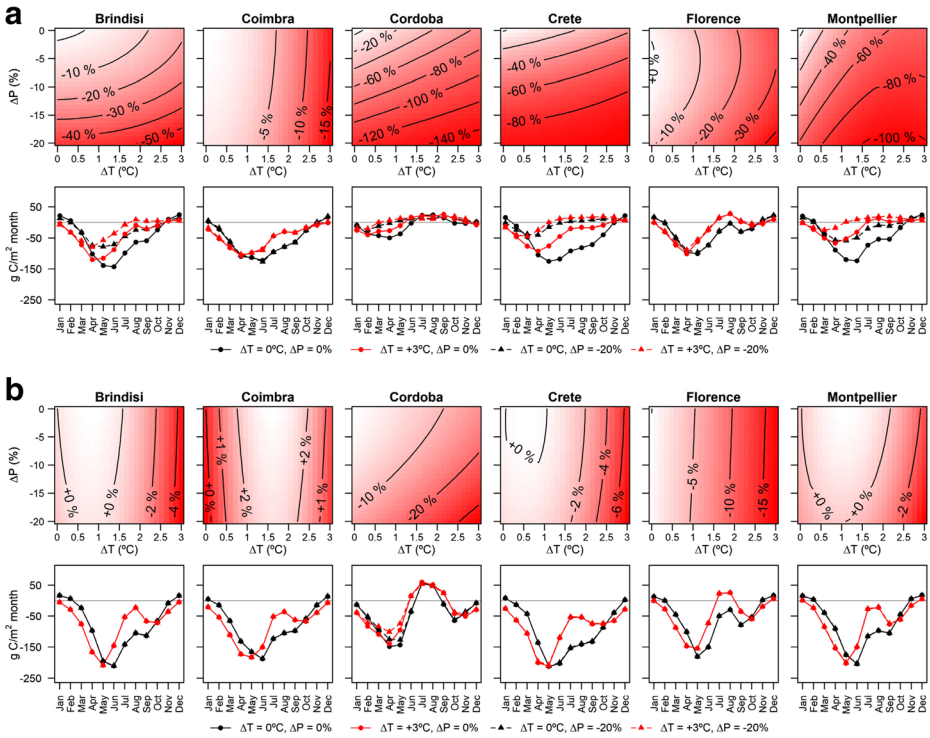


**Fig. 5** a IRSs of annual NEE in response to  $\Delta T$  and  $\Delta P$  changes and its monthly pattern under the baseline (filled line, black circles) and three extreme scenarios ( $\Delta T = 0\text{ }^{\circ}\text{C}$ ;  $\Delta P = -20\%$ ,  $\Delta T = +3\text{ }^{\circ}\text{C}$ ;  $\Delta P = 0\%$  and  $\Delta T = +3\text{ }^{\circ}\text{C}$ ;  $\Delta P = -20\%$ ) under EXT. **b** IRSs of annual NEE in response of  $\Delta T$  and  $\Delta P$  changes and its monthly pattern under the baseline (filled line, black circles) and three extreme scenarios ( $\Delta T = 0\text{ }^{\circ}\text{C}$ ;  $\Delta P = -20\%$ ,  $\Delta T = +3\text{ }^{\circ}\text{C}$ ;  $\Delta P = 0\%$  and  $\Delta T = +3\text{ }^{\circ}\text{C}$ ;  $\Delta P = -20\%$ ) under INT

The monthly pattern of NEE under baseline and three extreme scenarios ( $\Delta T = 0\text{ }^{\circ}\text{C}$ ;  $\Delta P = -20\%$ ,  $\Delta T = +3\text{ }^{\circ}\text{C}$ ;  $\Delta P = 0\%$  and  $\Delta T = +3\text{ }^{\circ}\text{C}$ ;  $\Delta P = -20\%$ ) is reported below each IRS in Fig. 5. These patterns showed that the highest C-uptake (usually in spring) occurred about 4 to 8 weeks earlier, depending on the level of air temperature increase, compared to the baseline. The stronger effect of increased temperature was found during the growing season (i.e., March–October), when a strong C-sequestration reduction was observed. By contrast, increased temperature contributed to a continuous C-uptake during winter, increasing NEE compared to the baseline. While temperature increase played a key role in determining variations in the monthly NEE pattern between baseline and the warmer scenarios, the rainfall decrease was the key driver for C-uptake reduction, influencing the magnitude especially in drier areas where the NEE turned into Reco during the summer. The joint effect of temperature increase and precipitation decrease exacerbated both monthly pattern and magnitude of NEE, resulting in an average C-sequestration loss of about 60% in all sites (Table S2).

The yearly mean values of olive grove NEE for intensive management (Fig. 5b) showed a different pattern of C-sequestration capacity from the baseline by increasing temperature and decreasing precipitation, compared to extensive management. A slight NEE increase between  $+1\text{ }^{\circ}\text{C}$  and  $+2.5\text{ }^{\circ}\text{C}$  was found at Coimbra, tending to decrease by reducing rainfall. A similar pattern was also observed at Brindisi, Crete, and Montpellier, where the NEE was maintained at the baseline value when temperatures were in a range between  $0$  and  $+1.5\text{ }^{\circ}\text{C}$ ,  $0$  and  $+1\text{ }^{\circ}\text{C}$ ,

and 0 and +2 °C, respectively. However, a slight decrease was observed both reducing precipitation and by approaching the extreme conditions ( $\Delta T = +3$  °C;  $\Delta P = -20\%$ ). The highest NEE reduction compared to the baseline was observed at Cordoba (-30%).

The monthly pattern of NEE still indicated that increased temperatures determined an advancement of the spring C-uptake peak and a NEE reduction during summer. However, under intensive management, the impact of increased temperature was highly compensated for by irrigation, which totally offset the rainfall decrease and also maintained the current yearly level of NEE. Irrigation was only unable to compensate for the impact of temperature on C-uptake at Cordoba, resulting in a reduction of spring C-uptake and an increase of summer respiration that tended to increase approaching the driest and warmest conditions. At Cordoba, both monthly pattern and magnitude of NEE were further influenced by the joint effect of temperature increase and precipitation decrease, resulting in a C-sequestration reduction of about 34% (Table S2). The yearly mean values of olive grove NPP for extensive management (Fig. 6a) showed a continuous decrease in productivity from the baseline, variable in magnitude among the sites by increasing temperature and decreasing precipitation. The highest NPP reductions observed under the extreme scenario ( $\Delta T = +3$  °C;  $\Delta P = -20\%$ ) was found at Montpellier (-70%), the lowest at Coimbra (-6%), and Florence (-15%). Cordoba and Crete showed similar patterns and NPP reductions (-60%). The IRSSs showed different shape among the sites.

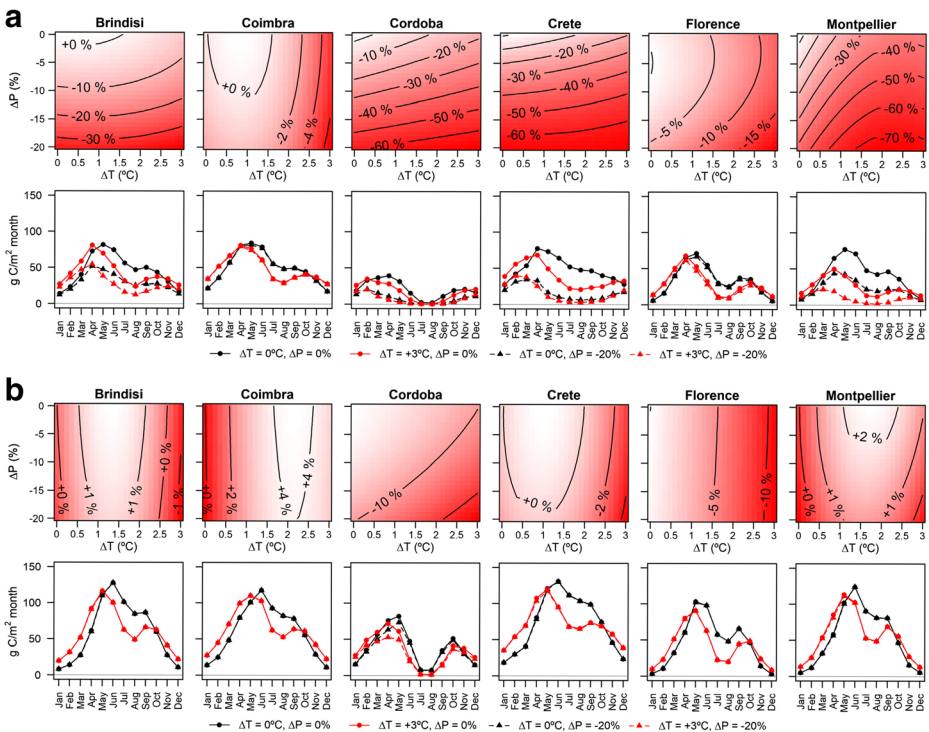


**Fig. 6** a IRSSs of annual NPP in response to  $\Delta T$  and  $\Delta P$  changes and its monthly pattern under the baseline (filled line, black circles) and three extreme scenarios ( $\Delta T = 0$  °C;  $\Delta P = -20\%$ ,  $\Delta T = +3$  °C;  $\Delta P = 0\%$  and  $\Delta T = +3$  °C;  $\Delta P = -20\%$ ) under EXT. b IRSSs of annual NPP in response to  $\Delta T$  and  $\Delta P$  changes and its monthly pattern under the baseline (filled line, black circles) and three extreme scenarios ( $\Delta T = 0$  °C;  $\Delta P = -20\%$ ,  $\Delta T = +3$  °C;  $\Delta P = 0\%$  and  $\Delta T = +3$  °C;  $\Delta P = -20\%$ ) under INT

Similarly to the monthly patterns of NEE, temperature increase played a key role at determining variations in the monthly NPP pattern between baseline and the warmer scenarios, while rainfall decrease was the key driver for C-uptake reduction. Generally, the magnitude of NPP decrease was lower than that observed for NEE, with the joint effect of temperature increase and precipitation decrease causing an average NPP reduction of about 45% at all sites (Table S2).

The yearly mean values of olive grove NPP for intensive management (Fig. 6b) showed a different pattern of C-sequestration capacity from the baseline by increasing temperature and decreasing precipitation compared to extensive management. A slight NPP increase by increasing temperature was observed at Brindisi, Coimbra, and Montpellier. The highest NPP increase was found at Coimbra (4%) when temperature increased between +2 and +2.5 °C. By contrast, the other sites showed a NPP decrease by increasing temperatures. Under the extreme scenario, the highest NPP decrease was observed at Cordoba (−15%) followed by Florence (−10%).

The monthly pattern confirmed that irrigation was able to compensate for the impact of rainfall reduction as well as partly limit the effect of temperature increase on productivity, allowing the current NPP level to be maintained in almost all sites. The highest yearly NPP decrease was observed at Cordoba and Florence—the warmer sites—where the temperature increase reduced C-uptake capacity during the whole growing season.

### 3.5 Global warming at +1.5 °C and +2 °C

Changes of NEE and NPP from the baseline to +1.5 and +2 °C warming and decreasing precipitation were found over all Mediterranean areas using both types of management (Table S3). These changes are described here considering only the current precipitation level (Table 3), given the low confidence in rainfall changes (timing and amount) under future scenarios (IPCC 2013). Under extensive management, the NEE strongly decreased from baseline (−4.83 tC ha<sup>−1</sup> year<sup>−1</sup>, on average) by −20.1 and −25.9% on average, under +1.5 and +2 °C ΔT, respectively. The highest NEE reduction at +2 °C was found at Montpellier (−56.9%), the lowest at Coimbra (−6.8%). Increasing temperature from +1.5 to +2 °C (Δ1.5–2 °C), the highest NEE decrease was found at Cordoba (−11%) and Crete (−7.5%). The NPP showed a similar pattern to baseline (4.7 tC ha<sup>−1</sup> year<sup>−1</sup>, on average) at +1.5 °C (−8.5%, on average) and +2 °C (−10.9%, on average) compared to NEE, with an overall decrease of 2.4%, on average. The highest NPP reduction at +2 °C was found at Montpellier (−34.4%), the lowest at Coimbra (−1%). Increasing temperature by +2 °C, the highest decrease was found at Cordoba, mostly driven by the reduced production. Generally, under extensive management, all six Mediterranean areas experienced a decrease in C-sequestration capacity and productivity when temperature increased from +1.5 to +2 °C, and this was amplified when precipitation was reduced.

A similar pattern was observed for intensive management where, however, irrigation strongly reduced the magnitude of warming impacts. Overall, the baseline NEE (−8.28 tC ha<sup>−1</sup> year<sup>−1</sup>, on average) and NPP (6.55 tC ha<sup>−1</sup> year<sup>−1</sup>, on average) decreased by 1.8 and 0% at +1.5 °C and 3.2 and 0.8% at +2 °C, respectively. The highest NEE reduction at +2 °C was found at Florence (−10.3%), while Coimbra experienced an increase of 2.6%. Increasing temperature from +1.5 to +2 °C, the highest decrease was found at Florence (3%). The highest NPP reduction at +2 °C was again observed at Florence (−6.4%), whilst Coimbra

**Table 3** Changes in NEE and NPP ( $tC/ha^{-1} year^{-1}$ ) from baseline to  $\Delta T = +1.5^{\circ}C$  and  $\Delta T = +2^{\circ}C$  warming and  $\Delta P = 0\%$  at 6 sites in the Mediterranean basin under EXT and INT.  $\Delta$ : 1.5–2  $^{\circ}C$  indicates changes of NEE and NPP moving from +1.5 to +2  $^{\circ}C$  (negative values indicate a worsening)

Management	Scenario	Brindisi	Coimbra	Cordoba	Creta	Florence	Montpellier	All-sites Avg.
NEE	EXT							
	Baseline ( $tC/ha^{-1} year^{-1}$ )	-5.94	-6.68	-1.20	-6.48	-3.62	-5.06	-4.83
	$\Delta T = +1.5^{\circ}C$ ; $\Delta P = 0\%$	-4.61%	-3.95%	-31.17%	-15.79%	-13.41%	-51.69%	-20.10%
INT	$\Delta T = +2^{\circ}C$ ; $\Delta P = 0\%$	-7.71%	-6.82%	-42.13%	-23.25%	-18.76%	-56.93%	-25.93%
	$\Delta$ 1.5–2 $^{\circ}C$	-3.10%	-2.88%	-10.96%	-7.46%	-5.35%	-5.24%	-5.83%
	Baseline ( $tC/ha^{-1} year^{-1}$ )	-9.15	-9.37	-5.04	-11.37	-6.52	-8.21	-8.28
	$\Delta T = +1.5^{\circ}C$ ; $\Delta P = 0\%$	+0.15%	+2.76%	-6.70%	-0.70%	-7.39%	+0.95%	-1.82%
	$\Delta T = +2^{\circ}C$ ; $\Delta P = 0\%$	-0.86%	+2.64%	-9.26%	-2.04%	-10.34%	+0.37%	-3.25%
	$\Delta$ 1.5–2 $^{\circ}C$	-1.01%	-0.12%	-2.57%	-1.34%	-2.95%	-0.58%	-1.43%
NPP	EXT							
	Baseline ( $tC/ha^{-1} year^{-1}$ )	5.41	5.95	2.39	5.77	3.97	4.72	4.70
	$\Delta T = +1.5^{\circ}C$ ; $\Delta T = 0\%$	+0.07%	+0.19%	-7.50%	-7.43%	-4.80%	-31.51%	-8.50%
INT	$\Delta T = +2^{\circ}C$ ; $\Delta T = 0\%$	-1.12%	-0.95%	-10.64%	-11.55%	-6.98%	-34.36%	-10.93%
	$\Delta$ 1.5–2 $^{\circ}C$	-1.19%	-1.14%	-3.14%	-4.12%	-2.19%	-2.85%	-2.44%
	Baseline ( $tC/ha^{-1} year^{-1}$ )	7.10	7.22	4.52	8.66	5.35	6.43	6.55
	$\Delta T = +1.5^{\circ}C$ ; $\Delta T = 0\%$	+1.56%	+3.83%	-4.11%	0.73%	-4.48%	+2.32%	-0.02%
	$\Delta T = +2^{\circ}C$ ; $\Delta T = 0\%$	+1.19%	+4.21%	-5.85%	-0.02%	-6.40%	+2.32%	-0.76%
	$\Delta$ 1.5–2 $^{\circ}C$	-0.37%	+0.37%	-1.74%	-0.75%	-1.92%	0.00%	-0.74%



experienced a considerable increase (4.2%). Increasing temperature from +1.5 to +2 °C, the highest decrease was found at Florence (1.9%).

## 4 Discussion

### 4.1 Model sensitivity, calibration, and validation

The most important parameters controlling plant growth and C-fluxes in DayCent were air temperature thresholds (optimal and maximum), number of soil layers influencing water and nutrient availability, and C-allocation within the different plant organs, in agreement with those identified by del Grosso et al. (2011), Rafique et al. (2013), and Necpalova et al. (2015). Concerning air temperature thresholds (Table S1), the calibration found the optimum and maximum temperature for olive tree production at 23 and 35 °C, respectively. These agree with studies suggesting the olive tree optimum in a 22–32 °C range, depending on the cultivation area (Carr 2014) and maximum thresholds above which physiological efficiency starts to reduce in the range 32–35 °C. More specifically, a considerable reduction in net photosynthesis was indicated at temperatures above 35–38 °C (Bongi and Long 1987; Marra 2009), while heat stresses leading to very detrimental conditions for the species can be observed when air temperatures exceed 40 °C (Carr 2014). Similarly, the optimum (18 °C) and maximum (26 °C) air temperature used for grass production are consistent with several native herbaceous species. The number of soil layers used to determine water and nutrient availability was calibrated by increasing the root depth from 30 to 75 cm. This reflected the findings by Rallo and Provenzano (2013), which indicated 0–0.75 m as the soil depth where 80% of roots are found. The biomass allocation was also consistent with results reported in the literature: the simulated above/belowground ratio was 0.27, close to that (0.3) found for olive orchard by Nardino et al. (2013); while the ratio between simulated growth and maintenance of tree respiration (0.24) was similar to that reported by Perez-Priego et al. (2014) for olive trees.

The calibration allowed assessing the reliability of DayCent at reproducing C-dynamics of the experimental olive grove (site 1), while the validation was needed for confirming that the calibrated parameters well reflected the olive ecophysiology when model was applied over different pedoclimatic and management conditions (site 2). The overall assessment of simulated olive grove C-dynamics indicated a substantial agreement with observed data. The model was capable of reproducing NEE, GPP, aboveground biomass, and yield under different conditions. As expected, the main modeling discrepancies were found simulating short-term C exchange fluctuations (del Grosso et al. 2011), while they were strongly reduced when the time-scale was expanded. In this study, the major discrepancies were found in spring, when agricultural practices such as tillage can modify both soil and ground vegetation, inducing higher ecosystem respiration due to oxidation of soil organic matter by increased bacterial activity (Pisante et al. 2015; Fiedler et al. 2016; Krauss et al. 2017), resulting in rapid changes in C emissions that can lead to minor uncertainties in C-flux partitioning. For instance, in 2011, the application of tillage in early spring in conjunction with a dry growing season (−40%) resulted in a prolonged period with lack of ground vegetation that may have reduced the capacity of the system to uptake C. This condition was not well reproduced by the model, where tillage induces changes on soil C and N emissions, water-filled pore space (WFPS), and soil organic carbon (SOC) content (del Grosso et al. 2005; Álvaro-Fuentes et al. 2017; Weiler et al. 2017; Wang et al. 2017), but it does not mimic the ground cover removal.

## 4.2 Future climate scenarios and alternative management practices

The results indicated a progressive decrease in C-sequestration capacity and productivity approaching extreme climate conditions, particularly when extensive management practices were used. Extensive management is adopted in the majority of olive groves, with traditional low-input plantations and wide plant density, few or no chemical inputs, no irrigation, and a more intensive weed control by soil tillage. The lack of agronomic and, hence, potential adaptation practices make the traditional groves highly responsive to climate variables. In fact NEE and NPP changes were particularly affected by precipitation, since water availability is the main limiting factor for vegetation activity in Mediterranean environments. In this study, the lower amounts of spring rainfall were at Crete (100.3 mm), Brindisi (136.4 mm), and Cordoba (139.8 mm), but the higher NEE decreases were observed at Cordoba (−120%), Crete (−8 0%), Montpellier (−60%), and Brindisi (−50%). This situation, which disagrees with the findings by Brillì et al. (2016), can be explained by the effect of air temperature exceeding the ecophysiological threshold determined for the species. When air temperature is above the maximum threshold at which photosynthesis takes place, physiological photoprotection mechanisms tend to decrease C-uptake until the system turns into a C-source, reducing yearly NEE and NPP (Camarero et al. 2012; Song et al. 2014). This decrease was considerable at Cordoba, where observed maximum mean monthly temperatures in July and August exceeded 35 °C, which is reported as the critical threshold above which olive tree production is reduced (Bongi and Long 1987; Marra 2009; Carr 2014). By contrast at Crete, where spring rainfall was lowest, the lower average monthly maximum temperature compared to Cordoba allowed a small but continuous C-sink even during the warmer period (i.e., summertime).

Increasing temperatures generally decreased NEE and NPP in all areas. This trend, varying in magnitude among the sites, was mainly associated with changes in seasonal activity (Figs. 5 and 6). The highest peak of NEE and NPP, usually observed in spring, was anticipated by about 4–8 weeks—depending on the level of air temperature increase—compared to the baseline. The peak also resulted as lower in magnitude since the optimum for olive groves shifted in a period when temperatures tend to rise quickly, thus shortening the period of highest vegetation activity. Increased temperature also led to low but continuous photosynthetic activity during winter. This pattern well reflected the reduction in the occurrence of winter photoinhibition and frost damage due to increased minimum temperature (Ogaya and Penuelas 2003). By contrast, increased temperature during summer may affect a wide number of metabolic processes such as respiration, meristem initiation, water transport, and phenology, including photosynthesis (Battaglia et al. 1996; Atkin and Tjoelker 2003; Ghannoum and Way 2011), resulting in a strong decrease of NEE and NPP compared to the baseline. Despite olive trees being able to survive under very dry conditions, thanks to ecophysiological mechanisms such as their inherent capacity to uptake water at high water potential and control stomata closure (Bongi et al. 1987; Fereres et al. 1996; Gucci and Caruso 2011; Sorrentino 2001), severe heat stress can lead to photosynthesis inhibition for prolonged periods (Fereres et al. 1996; Sorrentino 2001). When air temperatures are well above the critical threshold for photosynthesis, the respiration peak is found jointly with the starting point of photosynthesis decline, leading to minimum carbon gain (NEE) and reduced growth potential (NPP) (Lloyd and Farquhar 2008; Ghannoum and Way 2011). This is typical of Mediterranean species such as olive trees living close to their optimum temperature range (Saxe et al. 2001; Lloyd and Farquhar 2008; Werten et al. 2011).

Intensive management is generally used in olive groves to obtain high yields and maximum revenue. Under intensive management, irrigation plays a key role as it can reduce the competition between ground and tree vegetation for water and nutrients, thus maximizing the photosynthetic efficiency of the whole system (Villalobos et al. 2000; Tognetti et al. 2005). Under the simulated warming scenarios, this agronomic practice was able to compensate for NEE and NPP decrease in all rainfall reduction intervals over almost all areas. The only exception was Cordoba, where a yearly decrease of NEE (11.6%) and NPP (9.1%) was observed at  $\Delta P = -20\%$ . This decrease was mainly associated with low production during the period March–May (Fig. 6), suggesting the need to lengthen the period with no irrigation in those months. In the worst warming scenario, irrigation was unable to maintain the current level of NEE and NPP in sites with warmer summer temperature (i.e., Cordoba and Florence); however, it almost totally compensated for NEE and NPP losses in all other sites, also resulting in a slight increase in C-sequestration capacity and productivity at Coimbra (Table S2). Despite irrigation playing a fundamental role for limiting losses or maintaining current NEE and NPP levels, this agronomic practice is not economically viable. Currently, 50% of water consumption in the Mediterranean basin is for agriculture, with higher amounts in the driest regions (up to almost 90% in Syria, Egypt, Cyprus, and Greece) (FAO 2015). Future warming is expected to lead an increase in water use, with detrimental impacts especially in the hottest and developing sub-regions (Faurès et al., 2002), further exacerbated by related environmental issues such as groundwater over-exploitation and salinization (Souissi et al. 2013). For instance, about 85% of all water is consumed to produce food in Spain (Garrido et al. 2010); therefore, full irrigation in regions where olive grove cultivation is widespread (i.e., Andalusia) could add significant pressure to water basins (e.g., Guadalquivir basin) (Salmoral et al. 2011). Other concerns relate to farming system locations and information availability. For instance, in Italy, olive groves are usually cultivated on hilly and marginal areas far from water basins, making the use of irrigation difficult; moreover, information related to water supply timing and amounts should be more diffused and easily accessible. These issues raise important questions about the irrigated olive grove sustainability and its related business (e.g. transformation costs, selling price). Tools able to assess the olive grove response to water supply are needed to improve the knowledge on irrigation timing and amount, thus increasing its efficiency and reducing the overall costs. The potential of such tools should be exploited especially in the driest areas such as Cordoba, where expected changes in the olive grove ecophysiological pattern would be better addressed by scheduling the right amount and timing of water supply.

A comprehensive overview of the climate impacts at the two-headed temperature goals provided by the 2015 Paris Agreement is missing for several agroecosystems. In this study, results showed that moving from 1.5 to 2 °C could strongly impact olive groves. An overall increase of 2 °C can easily drive physiological temperatures above the maximum threshold indicated for the species (35 °C) in several Mediterranean areas. As shown, this increase would reduce the C-sequestration capacity and productivity of the whole system, especially during summertime. Under this condition, detrimental effects would be conceivable on ecosystem services such as reduced mitigation capacity (Brilli et al. 2016), increased presence of pathogens (Ponti et al. 2014), and reduced yield (Tupper 2012). Future warming may also lead to indirect losses in the olive oil and table olives market due to changes in product quality (Tupper 2012; Dag et al. 2014; Ponti et al. 2014; Ozdemir 2016). Although these issues can be partly compensated for by irrigation, the costs for its planning, systems building, and use (i.e., energy) would not be viable for the major grove areas, traditionally marginally located, and managed with low inputs.

This study has been focused on Mediterranean basin, a strategic economic, cultural, social, and environmental area touching three continents (Europa, Asia Africa). This area, projected to be more threatened by climate change, is globally the major where olive producers are located. Decreased olive grove mitigation capacity over the basin can more rapidly lead to warmer climate which in turn would require more adaptation. This should be focused especially to practices aimed at increasing soil water content or reducing evapotranspiration such as irrigation, grass cutting, mulching, etc. (Zhang et al. 2012; Andersen et al. 2013), which may play a key role at maintaining a suitable level of production and mitigation capacity in the next decades. These practices can allow the inter-linkages between mitigation and adaptation, which are essential and should not be considered as alternatives to each other but rather the best way to maintain a suitable level of production by reducing greenhouse gas emissions (Smith and Olesen 2010). Adaptation, however, would result in an increase of costs both to keep warming below the two degree target foreseen by Paris agreement (mitigation costs) or to reduce productivity losses (adaptation costs). Also, given the changed food demands and diets of the consumers, this cultivation is increasing attention within the global market (Xiong et al. 2014) and therefore impacts on these agro-ecosystems, especially when managed excluding any adaptation strategy, may have huge economic and social implications not only continental but also global.

## 5 Conclusion

The use of DayCent allowed CO<sub>2</sub> and energy fluxes to be investigated at a daily time scale thanks to the model's capability to reproduce the effect of tree canopy cover on grassland production, N competition between the two vegetation layers, and the effects of different agronomic practices driving C-dynamics. These abilities, used to improve the understanding of the responses of olive grove NEE and NPP to different environmental and anthropic factors in six Mediterranean sites, indicated a progressive decrease of uptake and productivity of olive groves approaching extreme climate conditions, particularly when extensive management was adopted. This decrease was also found to accelerate between 1.5 and 2 °C across all Mediterranean areas, confirming the findings of the IPCC AR5 Working Group 2 RFC assessment. However, adaptation measures devoted to soil water content increase (i.e., irrigation) can strongly reduce the decrease of both production and mitigation capacity.

Despite the DayCent model resulted to be a suitable tool for assessing the mitigative and productivity response of a Mediterranean olive grove ecosystem under future climate and different managements, further improvement of its structure is still needed. For instance, there is still an open debate about the sensitivity of SOC decomposition to soil increase temperatures, which cannot properly account in current first-kinetic models. In addition, other climate change impacts are not at all considered, such as the occurrence of pests and diseases on productivity. This latter aspect would be fundamental especially for predicting changes in risks of pathogens under future scenarios, where the expected increase of temperature and the changed pattern of precipitation may modify the pathogen presence and intensity (i.e., olive fly, olive knot, etc.) along the whole year. Finally, new field experiments considering specific adaptation and mitigation strategies are recommended to gain a broad overview about the role that olive groves can play under future conditions as well as to improve the reliability of future projections.

**Funding information** LIFE project “ADAPT2CLIMA” (Adaptation to Climate change Impacts on the Mediterranean islands’ Agriculture), no. LIFE14 CCA/GR/000928.

## References

- Abdalla M, Jones M, Yeluripati J, Smith P, Burke J, Williams M (2010) Testing DayCent and DNDC model simulations of N<sub>2</sub>O fluxes and assessing the impacts of climate change on the gas flux and biomass production from a humid pasture. *Atm Env* 44:2961–2970. <https://doi.org/10.1016/j.atmosenv.2010.05.018>
- Alvaro-Fuentes J, Easter M, Paustian K (2012) Climate change effects on organic carbon storage in agricultural soils of northeastern Spain. *Agric Ecosyst Environ* 155:87–94. <https://doi.org/10.1016/j.agee.2012.04.001>
- Álvaro-Fuentes J, Arrúe A, Bielsa C, Cantero-Martínez D, Plaza-Bonilla PK (2017) Simulating climate change and land use effects on soil nitrous oxide emissions in Mediterranean conditions using the Daycent model. *Agric Ecosyst Environ* 238:78–88. <https://doi.org/10.1016/j.agee.2016.07.017>
- Andersen L, Kühn BF, Bertelsen M, Bruus M, Larsen SE, Strandberg M (2013) Alternatives to herbicides in an apple orchard, effects on yield, earthworms and plant diversity. *Agric Ecosyst Environ* 172:1–5. <https://doi.org/10.1016/j.agee.2013.04.004>
- Atkin OK, Tjoelker MG (2003) Thermal acclimation and the dynamic response of plant respiration to temperature. *Trends Plant Sci* 8:343–351. [https://doi.org/10.1016/S1360-1385\(03\)00136-5](https://doi.org/10.1016/S1360-1385(03)00136-5)
- Baldocchi D, Valentini R, Running S (1996) Strategies for measuring and modeling carbon dioxide and water vapour fluxes over terrestrial ecosystem. *Glob Chang Biol* 2:159–168. <https://doi.org/10.1111/j.1365-2486.1996.tb00069.x>
- Battaglia M, Beadle C, Loughhead S (1996) Photosynthetic temperature responses of *Eucalyptus globosus* and *Eucalyptus nitens*. *Tree Physiol* 16:81–89 PMID: 14871750
- Bongi G, Long SP (1987) Light dependent damage to photosynthesis in olive trees during chilling and high temperatures stress. *Plant Cell Environ* 14:127–132. <https://doi.org/10.1111/1365-3040.ep11602267>
- Brilli L, Chiesi M, Maselli F, Moriondo M, Gioli B, Toscano P, Zaldei A, Bindi M (2013) Simulation of olive grove gross primary production by the combination of ground and multi-sensor satellite data. *Int J Appl Earth Obs* 23:29–36. <https://doi.org/10.1016/j.jag.2012.11.006>
- Brilli L, Gioli B, Toscano P, Moriondo M, Zaldei A, Cantini C, Ferrise R, Bindi M (2016) Rainfall regimes control C-exchange of Mediterranean olive orchard. *Agric Ecosyst Environ* 233:147–157. <https://doi.org/10.1016/j.agee.2016.09.006>
- Brilli L, Bechini L, Bindi M, Carozzi M, Cavalli D, Conant R, Dorich CD, Doro L, Ehrhardt F, Farina R, Ferrise R, Fitton N, Francaviglia R, Grace P, Iocola I, Klumpp K, Léonard J, Martin R, Massad RS, Recous S, Seddaiu G, Sharp J, Smith P, Smith WN, Soussana JF, Bellocchi G (2017) Review and analysis of strengths and weaknesses of agro-ecosystem models for simulating C and N fluxes. *Sci Total Environ* 598:445–470. <https://doi.org/10.1016/j.scitotenv.2017.03.208>
- Camarero JJ, Olano JM, Alfaro SJA, Fernández-Marín B, Becerril JM, García-Plazaola JI (2012) Photoprotection mechanisms in *Quercus ilex* under contrasting climatic conditions. *Flora* 207:557–564. <https://doi.org/10.1016/j.flora.2012.06.003>
- Carr MKV (2014) *Advances in irrigation agronomy: fruit crops*. Cambridge University Press, New York, p 350 ISBN: 9781107037359 ISBN-10: 1107037352
- Caruso G, Rapoport HF, Gucci R (2013) Long-term evaluation of yield components of young olive trees during the onset of fruit production under different irrigation regimes. *Irrig Sci* 31:37–47. <https://doi.org/10.1007/s00271-011-0286-0>
- Caruso G, Gucci R, Urbani S, Esposito S, Taticchi A, Di Maio I, Selvaggini R, Servili M (2014) Effect of different irrigation volumes during fruit development on quality of virgin olive oil of cv. Frantoio. *Agric Water Manag* 134:94–103. <https://doi.org/10.1016/j.agwat.2013.12.003>
- Chamizo S, Serrano-Ortiz P, Lopez-Ballesteros A, Sanchez-Canete EP, Vicente Vicente JL, Kowalsky AS (2017) Net ecosystem CO<sub>2</sub> exchange in an irrigated orchard of SE Spain: influence of weed cover. *Agric Ecosyst Environ* 239:51–64. <https://doi.org/10.1016/j.agee.2017.01.016>
- Chaves MM, Pereira JS, Maroco J, Rodrigues ML, Ricardo CPP, Osorio ML, Carvalho I, Faria T, Pinheiro C (2002) How plants cope with water stress in the field. Photosynthesis and growth. *Ann Bot* 89:907–916. <https://doi.org/10.1093/aob/mcf105>
- Collins M, Knutti R, Arblaster J, Dufresne JL, Fichefet T, Friedlingstein P, Gao X, Gutowski WJ, Johns T, Krinner G, Shongwe M, Tebaldi C, Weaver AJ, Wehner M (2013) Long-term climate change: projections, commitments and irreversibility. In: F T, Qin D, Plattner G-K, Tignor M, Allen SK, Boschung J, Nauels A, Xia Y, Bex V, Midgley PM (eds) *Climate change 2013: the physical science basis. Contribution of working group I to the fifth assessment report of the intergovernmental panel on climate change*. Cambridge University Press, Cambridge, UK and New York, NY, USA

- Dag A, Harlev G, Lavee S, Zipori I, Kerem Z (2014) Optimizing olive harvest time under hot climatic conditions of Jordan Valley, Israel. *Eur J Lipid Sci Technol* 116:169–176. <https://doi.org/10.1002/ejlt.201300211>
- de Gryze S, Wolf A, Kafka SR, Mitchell J, Rolston DE, Temple SR, Lee J, Six J (2010) Simulating greenhouse gas budgets of four California cropping systems under conventional and alternative management. *Ecol Appl* 20:1805–1819. <https://doi.org/10.1890/09-0772.1>
- del Grosso SJ, Parton WJ, Mosier AR, Hartman MD, Brenner J, Ojima DS, Schimel DS (2001a) Simulated interaction of carbon dynamics and nitrogen trace gas fluxes using the DAYCENT model. In: Schaffer M, Ma L, Hansen S (eds) *Modeling carbon and nitrogen dynamics for soil management*. CRC press, Florida, Boca Raton, pp 303–332
- del Grosso SJ, Parton WJ, Mosier AR, Hartman MD, Keough CA, Peterson GA, Ojima DS, Schimel DS (2001b) Simulated effects of land use, soil texture, and precipitation on N gas emissions using DAYCENT. In: Follett RF, F R, Hatfield JL (eds) *Nitrogen in the environment: sources, problems, and management*. Elsevier Science Publishers, Amsterdam, pp 413–431
- del Grosso SJ, Mosier AR, Parton WJ, Ojima DS (2005) DAYCENT model analysis of past and contemporary soil N<sub>2</sub>O and net greenhouse gas flux for major crops in the USA. *Soil Tillage Res* 83:9–24. <https://doi.org/10.1016/j.still.2005.02.007>
- del Grosso SJ, Parton WJ, Keough C, Reyes-Fox MA (2011). Special features of the DayCent modeling package and additional procedures for parameterization, calibration, validation, and applications. *Soil Science Society of America Special Publication Book Chapter* pp 155–176
- Ehrhardt F, Soussana J, Bellocchi G, Grace P, McAuliffe R, Recous S, Sandor R, Smith P, Snow V, Migliorati MD, Basso B, Bhatia A, Brilli L, Doltra J, Dorich CD, Doro L, Fitton N, Giacomini SJ, Grant B, Harrison MT, Jones SK, Kirschbaum MU, Klumpp K, Laville P, Leonard J, Liebig MA, Lieffering M, Martin R, Massad R, Meier E, Merbold L, Moore AD, Myrگیotis V, Newton P, Pattey E, Rolinski S, Sharp J, Smith WN, Wu L, Zhang Q (2018) Assessing uncertainties in crop and pasture ensemble model simulations of productivity and N<sub>2</sub>O emissions. *Glob Chang Biol* 24:603–616. <https://doi.org/10.1111/gcb.13965>
- FAO (2015). AQUASTAT Database. <http://www.fao.org/land-water/en/>. Accessed 1 May 2015
- Faurès JM, Hoogeveen J, Bruinsma J (2002) The FAO irrigated area forecast for 2030. Food and Agric. Organ, Rome
- Fereres E, Ruz C, Castro J, Gómez JA, Pastor M (1996). Recuperación del olivo después de una sequía extrema. Proceedings of the XIV. Congreso Nacional de Riegos, Aguadulce (Almería), 11–13 June, 1996, pp. 89–93
- Fiedler SR, Leinweber P, Jurasinski G, Eckhardt KU, Glatzel S (2016) Tillage-induced short-term soil organic matter turnover and respiration. *Soil* 2:475–486. <https://doi.org/10.5194/soil-2-475-2016>
- Fronzek S, Carter TR, Raisanen J, Ruokolainen L, Luoto M (2010) Applying probabilistic projections of climate change with impact models: a case study for sub-arctic palsa mires in Fennoscandia. *Clim Chang* 99:515–534. <https://doi.org/10.1007/s10584-009-9679-y>
- Gargouri K, Rigane H, Arous I, Touil F (2013) Evolution of soil organic carbon in an olive orchard under arid climate. *Sci Hortic* 152:102–108. <https://doi.org/10.1016/j.scienta.2012.11.025>
- Garrido A, Llamas MR, Varela-Ortega C, Novo P, Rodríguez Casado R, Aldaya MM (2010). Water footprint and virtual water trade in Spain. Policy implications. Fundación Marcelino Botín. Springer. p 153
- Ghannoum O, Way DA (2011) On the role of ecological adaptation and geographic distribution in the response of trees to climate change. *Tree Physiol* 31:1273–1276. <https://doi.org/10.1093/treephys/tpr115>
- Giorgi F, Lionello P (2008) Climate change projections for the Mediterranean region. *Glob Planet Chang* 63:90–104. <https://doi.org/10.1016/j.gloplacha.2007.09.005>
- Graux AI, Soussana JF, Brisson N, Hill D, Lardy R (2009) Modelling climate change impacts on grasslands and possible adaptations of livestock systems. *Climate Change: Global Risks, Challenges and Decisions IOP Conf. Series: Earth Environ Sci* 6:242046. <https://doi.org/10.1088/1755-1307/6/4/242046>
- Graux AI, Bellocchi G, Lardy R, Soussana JF (2013) Ensemble modelling of climate change risks and opportunities for managed grasslands in France. *Agric For Meteorol* 170:114–131. <https://doi.org/10.1016/j.agrformet.2012.06.010>
- Gucci R, Caruso G (2011) Environmental stress and sustainable olive growing. Proceeding of the XXVII international horticultural congress on science and horticulture for people, Lisboa 2010. *Acta Hortic* 924: 19–30
- Gucci R, Caruso G, Bertolla C, Urbani S, Taticchi A, Esposto S, Servili M, Sifola MI, Pellegrini S, Pagliai M, Vignozzi N (2012) Changes in soil properties and tree performance induced by soil management in a high-density olive orchard. *Eur J Agron* 41:18–27. <https://doi.org/10.1016/j.eja.2012.03.002>
- IPCC (2013) *Climate Change 2013: The physical science basis*. Contribution of working group I to the fifth assessment report of the intergovernmental panel on climate change. In: Qin TF,D, Plattner G-K, Tignor M, Allen SK, Boschung J, Nauels A, Xia Y, Bex V, Midgley PM (eds) . Cambridge University Press, Cambridge, UK and New York, USA, p 1535

- Jia X, Zha TS, Wu B, Zhang YQ, Gong JN, Qin SG, Chen GP, Kellomäki S, Peltola H (2014) Biophysical controls on net ecosystem CO<sub>2</sub> exchange over a semiarid shrubland in Northwest China. *Biogeosci Discuss* 11:5089–5122. <https://doi.org/10.5194/bgd-11-5089-2014>
- Krauss M, Ruser R, Müller T, Hansen S, Mäder P, Gattinger A (2017) Impact of reduced tillage on greenhouse gas emissions and soil carbon stocks in an organic grass-clover ley - winter wheat cropping sequence. *Agric Ecosyst Environ* 239:324–333. <https://doi.org/10.1016/j.agee.2017.01.029>
- Kwon H, Pendall E, Ewers BE, Cleary M, Naithani K (2008) Spring drought regulates summer net ecosystem CO<sub>2</sub> exchange in a sagebrush-steppe ecosystem. *Agr For Met* 148:381–391. <https://doi.org/10.1016/j.agrformet.2007.09.010>
- Lenth RV (2009) Response-surface methods in R, using rsm. *J Stat Softw* 32:1–17. <https://doi.org/10.18637/jss.v032.i07>
- Lloyd J, Farquhar GD (2008) Effects of rising temperatures and [CO<sub>2</sub>] on the physiology of tropical forest trees. *Philos Trans R Soc B* 363:1811–1817. <https://doi.org/10.1098/rstb.2007.0032>
- Lugato E, Leip A, Jones A (2018) Mitigation potential of soil carbon management overestimated by neglecting N<sub>2</sub>O emissions. *Nat Clim Chang* 8:219–223 <https://www.nature.com/articles/s41558-018-0087-z>
- Lugato E, Panagos P, Bampa F, Jones A, Montanarella L (2014) A new baseline of organic carbon stock in European agricultural soils using a modelling approach. *Glob Chang Biol* 20:313–326. <https://doi.org/10.1111/gcb.12292>
- Lugato E, Zuliani M, Alberti G, Delle Vedove G, Gioli B, Miglietta F, Peressotti A (2010) Application of DNDC biogeochemistry model to estimate greenhouse gas emissions from Italian agricultural areas at high spatial resolution. *Agric Ecosyst Environ* 139:546–556. <https://doi.org/10.1016/j.agee.2010.09.015>
- Marra FP (2009) Ambiente di Coltivazione. In: Pisante M, Inglese P, Lercker G (eds) *L'Ulivo e l'Olio*. Città di Castello (PG). ART S.p.A. Ed. Script, Bologna, pp 350–357
- Maselli F, Chiesi M, Brill L, Moriondo M (2012) Simulation of olive yield in Tuscany through the integration of remote sensing and ground data. *Ecol Model* 244:1–12. <https://doi.org/10.1016/j.ecolmodel.2012.06.028>
- Medrano H, Flexas J, Galmés J (2009) Variability in water use efficiency at the leaf level among Mediterranean plants with different growth forms. *Plant Soil* 317:17–29. <https://doi.org/10.1007/s11104-008-9785-z>
- Mohamad RS, Bteich MR, Cardone G, Marchini A (2013) Economic analysis in organic olive farms: the case of the ancient olive trees in the rural parkland in Apulia. *New Medit* 12:55–61
- Montanaro G, Nuzzo V, Xiloyannis C, Dichio B (2018) Climate change mitigation and adaptation in agriculture: the case of olive. *J Water Clim Chang*. <https://doi.org/10.2166/wcc.2018.023>
- Moriondo M, Ferrise R, Trombi G, Brilli L, Dibari C, Bindi M (2015) Modelling olive trees and grapevines in a changing climate. *Environ Model Softw* 72:387–401. <https://doi.org/10.1016/j.envsoft.2014.12.016>
- Nardino M, Pernice F, Rossi F, Georgiadis T, Facini O, Motisi A, Drago A (2013) Annual and monthly carbon balance in an intensively managed Mediterranean olive orchard. *Photosynthetica* 51:63–74. <https://doi.org/10.1007/s11099-012-0079-6>
- Necpálová M, Anex RP, Fienen MN, del Grosso SJ, Castellano MJ, Sawyer JE, Iqbal J, Pantoja JL, Barker DW (2015) Understanding the DayCent model: calibration, sensitivity, and identifiability through inverse modeling. *Environ Model Softw* 66:110–130. <https://doi.org/10.1016/j.envsoft.2014.12.011>
- Nieto OM, Castro J, Fernández E, Smith P (2010) Simulation of soil organic carbon stocks in a Mediterranean olive grove under different soil-management systems using the RothC model. *Soil Use Manag* 26:118–125. <https://doi.org/10.1111/j.1475-2743.2010.00265.x>
- Noy-Meir I (1973) Desert ecosystems: environment and producers. *Annu Rev Ecol Syst* 4:25–51. <https://doi.org/10.1146/annurev.es.04.110173.000325>
- Ogaya R, Penuelas J (2003) Comparative field study of *Quercus ilex* and *Phillyrea latifolia*: photosynthetic response to experimental drought conditions. *Environ Exp Bot* 50:137–148. [https://doi.org/10.1016/S0098-8472\(03\)00019-4](https://doi.org/10.1016/S0098-8472(03)00019-4)
- Oxfam (2010) The road to olive farming: challenges to developing the economy of olive oil in the West Bank. ISBN: 9781848147577. Available at: [https://www.oxfam.org/sites/www.oxfam.org/files/the-road-to-olive-farming\\_0.pdf](https://www.oxfam.org/sites/www.oxfam.org/files/the-road-to-olive-farming_0.pdf)
- Ozdemir Y (2016) Effects of climate change on olive cultivation and table olive and olive oil quality. *Scientific Papers, Horticulture Vol. LX*, 2016. ISSN 2286–1580, ISSN-L 2285–5653
- Parton WJ, Schimel DS, Ojima D, Cole CV (1994) A general model for soil organic matter dynamics: sensitivity to litter chemistry, texture and management. In: Bryant RB, Arnoldm RW (eds) *Quantitative Modeling of Soil Forming Processes*. Soil Science Society of America, Madison, pp 147–167. <https://doi.org/10.2136/sssaspepub39.c9>
- Parton WJ, Hartman M, Ojima D, Schimel D (1998) DAYCENT and its land surface submodel: description and testing. *Glob Planet Chang* 19:35–48. [https://doi.org/10.1016/S0921-8181\(98\)00040-X](https://doi.org/10.1016/S0921-8181(98)00040-X)
- Pérez-Priego O, Testi L, Kowalski AS, Villalobos FJ, Orgaz F (2014) Aboveground respiratory CO<sub>2</sub> effluxes from olive trees (*Olea europaea* L.). *Agrofor Syst* 88:245–255. <https://doi.org/10.1007/s10457-014-9672-y>

- Pirttioja N, Carter T, Fronzek S, Bindi M, Hoffmann H, Palosuo T, Ruiz-Ramos M, Tao F, Trnka M, Acutis M, Asseng S, Baranowski P, Basso B, Bodin P, Buis S, Cammarano D, Deligios P, Destain M, Dumont B, Ewert F, Ferrise R, François L, Gaiser T, Hlavinka P, Jacquemin I, Kersebaum K, Kollas C, Krzyszczak J, Lorite I, Minet J, Minguéz M, Montesino M, Moriondo M, Müller C, Nendel C, Öztürk I, Perego A, Rodríguez A, Ruane A, Ruget F, Sanna M, Semenov M, Slawinski C, Stratonovitch P, Supit I, Waha K, Wang E, Wu L, Zhao Z, Rötter R (2015) Temperature and precipitation effects on wheat yield across a European transect: a crop model ensemble analysis using impact response surfaces. *Clim Res* 65:87–105. <https://doi.org/10.3354/cr01322>
- Pisante M, Stagnari F, Acutis M, Bindi M, Brilli L, Di Stefano V, Carozzi M (2015) Conservation agriculture and climate change. In: Farooq M, Siddique K (eds). Springer, pp 579–620. [https://doi.org/10.1007/978-3-319-11620-4\\_22](https://doi.org/10.1007/978-3-319-11620-4_22)
- Ponti L, Gutierrez AP, Ruti PM, Dell'Aquila A (2014) Fine-scale ecological and economic assessment of climate change on olive in the Mediterranean Basin reveals winners and losers. *PNAS* 111:5598–5603. <https://doi.org/10.1073/pnas.1314437111>
- Prabhakaran Nair KP (2010) The agronomy and economy of important tree crops of the developing world. Elsevier, India, p 368 ISBN: 978-0-12-384677-8
- Rafique R, Fienen MN, Parkin TB, Anex RP (2013) Nitrous oxide emissions from cropland: a procedure for calibrating the DayCent biogeochemical model using inverse modelling. *Water Air Soil Pollut* 224:1677. <https://doi.org/10.1007/s11270-013-1677-z>
- Rallo G, Provenzano G (2013) Modelling eco-physiological response of table olive trees (*Olea europaea* L.) to soil water deficit conditions. *Agr Water Manag* 120:79–88. <https://doi.org/10.1016/j.agwat.2012.10.005>
- Reichstein M, Falge E, Baldocchi D, Papale D, Aubinet M, Berbigier P, Bernhofer C, Buchmann N, Gilmanov T, Granier A, Grunwald T, Havrankova K, Ilvesniemi H, Dalibor J, Knohl A, Laurila T, Lohila A, Loustau D, Matteucci G, Meyer T, Miglietta F, Ourcival JM, Pumpanen J, Rambal S, Rotenberg E, Sanz MJ, Tenhunen J, Seufert G, Vaccari F, Vesala T, Valentini R (2005) On the separation of net ecosystem exchange into assimilation and ecosystem respiration: review and improved algorithm. *Glob Chang Biol* 11:1424–1429. <https://doi.org/10.1111/j.1365-2486.2005.001002.x>
- Ruiz-Ramos M, Ferrise R, Rodríguez A, Lorite I, Bindi M, Carter TR, Fronzek S, Palosuo T, Pirttioja N, Baranowski P, Buis S, Cammarano D, Chen Y, Dumont B, Ewert F, Gaiser T, Hlavinka P, Hoffmann H, Höhn JG, Jurecka F, Kersebaum KC, Krzyszczak J, Lana M, Mechiche-Alami A, Minet J, Montesino M, Nendel C, Porter JR, Ruget F, Semenov M, Steinmetz Z, Stratonovitch P, Supit I, Tao F, Trnka M, de Wit A, Rötter RP (2018) Adaptation response surfaces for local management of wheat under perturbed climate and CO<sub>2</sub> concentration in a Mediterranean environment. *Agric Syst* 159:260–274. <https://doi.org/10.1016/j.agsy.2017.01.009>
- Salmoral G, Aldaya MM, Chico D, Garrido A, Llama MR (2011) The water footprint of olives and olive oil in Spain. *Span J Agric Res* 9:1089–1104. <https://doi.org/10.5424/sjar.20110904-035-11>
- Sándor R, Barcza Z, Hidy D, Lellei-Kovács E, Ma S, Bellocchi G (2016) Modelling of grassland fluxes in Europe: evaluation of two biogeochemical models. *Agric Ecosyst Environ* 215:1–19. <https://doi.org/10.1016/j.agee.2015.09.001>
- Saxe H, Cannell MGR, Johnsen Ø, Ryan MG, Vourlitis G (2001) Trees and forest functioning in response to global warming. *New Phytol* 149:369–400. <https://doi.org/10.1046/j.1469-8137.2001.00057.x>
- Scandellari F, Caruso G, Liguori G, Meggio F, Palese AM, Zanotelli DG, Celano G, Gucci R, Inglesse P, Pitacco A, Tagliavini M (2016) A survey of carbon sequestration potential of orchards and vineyards in Italy. *Eur J Hort Sci* 81:106–114. <https://doi.org/10.17660/eJHS.2016/81.2.4>
- Semenov MA, Barrow EM (1997) Use of a stochastic weather generator in the development of climate change scenarios. *Climate Change* 35:397–414. <https://doi.org/10.1023/A:1005342632279>
- Semenov M, Stratonovitch P (2010) Use of multi-model ensembles from global climate models for assessment of climate change impacts. *Clim Res* 41:1–14. <https://doi.org/10.3354/cr00836>
- Smith P, Olesen JE (2010) Synergies between the mitigation of, and adaptation to, climate change in agriculture. *J Agric Sci* 148:543–552. <https://doi.org/10.1017/S0021859610000341>
- Smith WN, Desjardins RL, Grant B, Li C, Lemke R, Rochette P, Corre MD, Pennock D (2002) Testing the DNDC model using N<sub>2</sub>O emissions at two experimental sites in Canada. *Can J Soil Sci* 82:365–374. <https://doi.org/10.4141/S01-048>
- Sofó A, Nuzzo V, Palese AM, Xiloyannis C, Celano G, Zukowskyj P, Dichio B (2005) Net CO<sub>2</sub> storage in Mediterranean olive and peach orchards. *Hortic Sci* 107:17–24. <https://doi.org/10.1016/j.scienta.2005.06.001>
- Soil Survey Staff (2010) Keys to Soil Taxonomy. 11th Edition, USDA-NRCS, Washington DC
- Song Y, Chen Q, Ci D, Shao X, Zhang D (2014) Effects of high temperature on photosynthesis and related gene expression in poplar. *BMC Plant Biol* 14:111. <https://doi.org/10.1186/1471-2229-14-111>



- Sorrentino G (2001). Meccanismi fisiologici di recupero dal deficit idrico in Olivo. In: Gestione dell'acqua e del territorio per un'olivicultura sostenibile. Atti del corso internazionale di aggiornamento tecnico-scientifico, Napoli 24–28 settembre 2001, pp. 103–119
- Souissi I, Temani N, Belhouchette H (2013) Vulnerability of Mediterranean agricultural systems to climate: from regional to field scale analysis. In: Pielke RA Sr (ed) Climate Vulnerability, Understanding and addressing threats to essential resources. Elsevier, Amsterdam, The Netherlands, Oxford, UK, Burlington, USA, pp 89–103. <https://doi.org/10.1016/B978-0-12-384703-4.00221-5>
- Testa R, Di Trapani AM, Sgroi F, Tudisca S (2014) Economic analysis of process innovations in the management of olive farms. *Am J Appl Sci* 11:1486–1491. <https://doi.org/10.3844/ajassp.2014.1486.1491>
- Tognetti R, d'Andria R, Morelli G, Alvino A (2005) The effect of deficit irrigation on seasonal variations of plant water use in *Olea europaea* L. *Plant Soil* 273:139–155. <https://doi.org/10.1007/s11104-004-7244-z>
- Tonitto C, David MB, Drinkwater EL, Li C (2007) Application of the DNDC model to tile-drained Illinois agroecosystems: model calibration, validation, and uncertainty analysis. *Nutr Cycl Agroecosyst* 78:51–63. <https://doi.org/10.1007/s10705-006-9076-0>
- Tupper N (2012) Spanish olive oil under constant threat from climate change. *Olive Oil Times*, October 26
- UNFCCC (2015) Adoption of the Paris Agreement FCCC/CP/2015/L9/Rev.1
- Villalobos FJ, Orgaz F, Testi L, Fereres E (2000) Measurement and modeling of evapotranspiration of olive (*Olea europaea* L.) orchards. *Eur J Agron* 13:155–163. [https://doi.org/10.1016/S1161-0301\(00\)00071-X](https://doi.org/10.1016/S1161-0301(00)00071-X)
- Villalobos FJ, Testi L, Hidalgo J, Pastor M, Orgaz F (2006) Modelling potential growth and yield of olive (*Olea europaea* L.) canopies. *Eur J Agron* 24:296–303. <https://doi.org/10.1016/j.eja.2005.10.008>
- Vital JA, Gaurut M, Lardy R, Viovy N, Soussana JF, Bellocchi G, Martin R (2013) High-performance computing for climate change impact studies with the pasture simulation model. *Comput Electron Agric* 98:131–135. <https://doi.org/10.1016/j.compag.2013.08.004>
- Xiong B, Sumner D, Matthews W (2014) A new market for an old food: the U.S. demand for olive oil. *Agric Econ* 45:107–118. <https://doi.org/10.1111/agec.12133>
- Wang Y, Dou F, Storlien JO, Wight JP, Paustian KH, del Grosso SJ, Hons FM (2017). Simulating impacts of bioenergy Sorghum residue return on soil organic carbon and greenhouse gas emissions using the DAYCENT model. In: Field D.J., Morgan C.L.S., McBratney A.B. (eds.) *Global soil security. Progress in Soil Science*. Springer, Cham
- Weiler DA, Tomquist CG, Parton W, dos Santos HP, Santi A, Bayer C (2017) Crop biomass, soil carbon, and nitrous oxide as affected by management and climate: a DayCent application in Brazil. *Soil Sci Soc Am J* 81: 945–955. <https://doi.org/10.2136/sssaj2017.01.0024>
- Wartin TM, McGuire MA, Teskey RO (2011) Higher growth temperatures decreased net carbon assimilation and biomass accumulation of northern red oak seedlings near the southern limit of species range. *Tree Physiol* 31:1277–1288. <https://doi.org/10.1093/treephys/tpr091>
- Wu CFJ, Hamada M (2009) *Experiments: planning, analysis, and parameter design optimization*, 2nd Edition. BWSTM, 760 pages. ISBN-10: 0471699462 ISBN-13: 978-0471699460
- Zhang Y, Xu M, Chen H, Adams J (2009) Global pattern of NPP to GPP ratio derived from MODIS data: effects of ecosystem type, geographical location and climate. *Glob Ecol Biogeogr* 18:280–290. <https://doi.org/10.1111/j.1466-8238.2008.00442.x>
- Zhang FY, Wu PT, Zhao XN, Cheng XF (2012) Water-saving mechanisms of intercropping system in improving cropland water use efficiency. PMID 23:1400–1406 22919855
- Zhou X, Brandle JR, Schoeneberger MM, Awada T (2007) Developing above ground woody biomass equations for open-grown, multiple-stemmed tree species: shelterbelt-grown Russian-olive. *Ecol Model* 202:311–323. <https://doi.org/10.1016/j.ecolmodel.2006.10.024>